Inorganic Chemistry
Article

Inorg. Chem. **2009**, *48*, 9385–9392 **9385**
DOI: 10.1021/ic9013015

Single-Electron Transfer in Palladium Complexes of 1,4-Naphthoquinone-Containing Bis(pyrazol-1-yl)methane Ligands

Sebastian Scheuermann,[†] Biprajit Sarkar,[‡] Michael Bolte,[†] Jan W. Bats,[§] Hans-Wolfram Lerner,[†] and Matthias Wagner*[,†]

[†]*Institut für Anorganische und Analytische Chemie, Goethe-Universität Frankfurt, Max-von-Laue-Strasse 7, D-60438 Frankfurt (Main), Germany,* [‡]*Institut für Anorganische Chemie, Universität Stuttgart, Pfaffenwaldring 55, D-70569 Stuttgart, Germany, and* [§]*Institut für Organische Chemie, Goethe-Universität Frankfurt, Max-von-Laue-Strasse 7, D-60438 Frankfurt (Main), Germany*

Received July 7, 2009

A 1,4-naphthoquinone-substituted bis(pyrazol-1-yl)methane ligand (N^N) has been synthesized and transformed into its corresponding Pd^{II} chelate complex [(N^N)$PdCl_2$]. Both N^N and [(N^N)$PdCl_2$] have been fully characterized by NMR spectroscopy, spectro-electrochemistry, and X-ray crystallography. After treatment of [(N^N)$PdCl_2$] with NEt_3, the signature of a 1,4-naphthosemiquinonate radical is visible in the UV−vis- and electron paramagnetic resonance (EPR) spectrum of the reaction mixture; the free ligand N^N does not react with NEt_3 under the conditions applied. It is therefore concluded that NEt_3 first reduces the Pd^{II}-ion of [(N^N)$PdCl_2$] to the zero-valent state and that this reaction is followed by a single-electron transfer from the metal atom to the 1,4-naphthoquinone moiety. The complex has been specifically designed to disfavor any direct Pd-to-naphthoquinone coordination. Electron transfer thus proceeds through space or, less likely, via σ-bonds of the ligand framework.

Introduction

The selective catalytic oxidation of organic compounds represents a fundamental problem of synthetic chemistry and an economically important challenge.

One of the major breakthroughs in this area was the discovery of the Pd^{II}-initiated oxidation of ethylene to acetaldehyde, which is performed on an industrial scale (Wacker oxidation).[1] In this process, Pd^{II} first coordinates the olefin, then mediates the nucleophilic attack of H_2O to the double bond, and finally accepts two electrons from the substrate. In subsequent studies, the system Pd^{II}/Pd^0 also proved successful for the preparation of numerous heterocycles via the intramolecular addition of alcohols[2] or amine derivatives[3] to appropriately substituted olefins.

The precious Pd^{II}-salt either has to be used in stoichiometric amounts,[4,5] or, to close a catalytic cycle, Pd^0 needs to be reoxidized. Even though precedence exists for the direct oxidation of Pd^0 to Pd^{II} by air (O_2),[6,7] this reaction is often difficult to achieve because the corresponding energy barrier tends to be higher than that for catalyst decomposition (i.e., precipitation of Pd black).[8] In the case of the Wacker process, the problem has been solved elegantly by employing $CuCl_2$ as redox catalyst.[1] Later on, it was even possible to extend the reaction protocol ($PdCl_2$, $CuCl_2$, O_2; mixture of a polar solvent and H_2O) to the aerobic oxidation of a large variety of alkenes.[8] However, a drawback is that the presence of chloride ions, which are required to stabilize the system, lowers the rate of the reaction,[9] and can lead to the formation of chlorinated byproducts.[10,11]

As a consequence, there is an ongoing quest for modified catalyst formulations. The combination of palladium acetate ([$Pd(OAc)_2$]) with 1,4-benzoquinone (BQ) as oxidizing agent turned out to be a viable chloride-free alternative − not only for the transformation of alkenes into carbonyl compounds but also for the 1,4-diacetoxylation of 1,3-dienes.[8] In many of these syntheses, stoichiometric quantities of BQ are consumed[5] because, in contrast to the $CuCl_2/CuCl$ couple, the aerobic reoxidation of 1,4-hydroquinone (HQ) to BQ is very slow under the reaction conditions applied.[8] Thus, to be able

*To whom correspondence should be addressed. E-mail: matthias.wagner@chemie.uni-frankfurt.de.

(1) Smidt, J.; Hafner, W.; Jira, R.; Sedlmeier, J.; Sieber, R.; Rüttinger, R.; Kojer, H. *Angew. Chem.* **1959**, *71*, 176–182.
(2) Hosokawa, T.; Murahashi, S.-I. *Acc. Chem. Res.* **1990**, *23*, 49–54.
(3) Müller, T. E.; Beller, M. *Chem. Rev.* **1998**, *98*, 675–703.
(4) Phillips, F. C. *Am. Chem. J.* **1894**, *16*, 255–277.
(5) Hegedus, L. S.; Allen, G. F.; Bozell, J. J.; Waterman, E. L. *J. Am. Chem. Soc.* **1978**, *100*, 5800–5807.
(6) ten Brink, G.-J.; Arends, I. W. C. E.; Sheldon, R. A. *Science* **2000**, *287*, 1636–1639.
(7) Stahl, S. S. *Angew. Chem., Int. Ed.* **2004**, *43*, 3400–3420.
(8) Piera, J.; Bäckvall, J.-E. *Angew. Chem., Int. Ed.* **2008**, *47*, 3506–3523.
(9) Henry, P. M. *J. Am. Chem. Soc.* **1964**, *86*, 3246–3250.
(10) Stangl, H.; Jira, R. *Tetrahedron Lett.* **1970**, *11*, 3589–3592.
(11) van Leeuwen, P. W. N. M. *Homogeneous Catalysis. Understanding the Art*; Kluwer Academic Publishers: Dordrecht, Boston, London, 2004.

Published on Web 09/01/2009

to use O_2 as the final oxidizing agent, a second redox catalyst is required to accelerate the regeneration of BQ. A number of different redox-active compounds have shown promising potential in this respect, among them nitrogen oxides,[12] (hetero)polyoxometallates,[13] and transition metal complexes with macrocyclic ligands (e.g., iron phthalocyanine,[14] cobalt tetraphenylporphyrin,[14] cobalt salenes[15]). The most recent developments in this area are focusing on hybrid redox catalysts in which 1,4-quinone moieties are covalently tethered to cobalt salene or cobalt porphyrine complexes to increase the overall efficiency of the electron transfer from Pd^0 to O_2.[16−18]

Our group has a long-standing interest in electron-transfer processes that occur within transition metal complexes with redox-active (particularly BQ/HQ-containing) ligands.[19−28] In this context, the reoxidation of Pd^0 by BQ provides a particularly interesting problem because it has been assumed that a direct coordination of the olefinic double bond(s) of the BQ molecule to the Pd^0-atom takes place, which not only stabilizes Pd^0 against the formation of Pd black but also promotes the desired metal-to-ligand electron transfer.[29,30] The question thus arises, whether the formation of a Pd^0-BQ complex is a prerequisite for a successful reoxidation process, or whether the electrons can also be transferred via a through-space pathway. To answer this question, we have prepared the Pd^{II}-complex of a 1,4-quinone-substituted bis(pyrazol-1-yl)methane ligand which had been specifically designed to prohibit any covalent intra- or intermolecular interaction between the metal center and the organic redox system. The Pd^{II}-ion was then selectively reduced to its Pd^0-state, and the follow-up reactions were monitored by UV−vis- as well as EPR spectroscopy. Herein, we describe the results of these investigations and provide evidence for a through-space single-electron transfer from Pd^0 to the ligand, resulting in the formation of a semiquinonate radical.

Results and Discussion

Complex **5** (Scheme 1) was developed as the key molecule for our projected studies on the basis of the following considerations: (i) Bis(pyrazol-1-yl)methane is supposed to be a sufficiently strong chelator to prevent metal ion leaching even in strongly coordinating solvents and at elevated temperatures. (ii) 1,4-Naphthoquinone (NQ) was selected (instead of 1,4-benzoquinone) as redox-active unit because it possesses only one alkene moiety able to engage in Pd^0-coordination.[31] Since this C=C double bond is sterically protected in **5**, an unwanted direct Pd-NQ coordination seems highly unlikely. (iii) It is well-known that the methylene protons of bis(pyrazol-1-yl)methanes are rather acidic, which has been exploited for further derivatization of the ligand,[32] but can also lead to unwanted side reactions already under mild basic conditions.[28] The carbon atom bearing the two pyrazol-1-yl substituents was therefore methylated with the aim to increase the base-stability of the ligand.

Synthesis and Spectroscopy. The synthesis of complex **5** is summarized in Scheme 1. First, the bis(pyrazol-1-yl)-methane derivative **2** was prepared in yields of about 85% from 1,4-dimethoxy-2-naphthalenecarboxaldehyde (**1**[33]) and bis(pyrazol-1-yl)methanone[34] (pz_2CO; 1 equiv) in the presence of a catalytic amount of anhydrous $CoCl_2$.[34−36]

To replace the acidic methylene proton of **2** by a less reactive methyl group, **2** was treated with *n*BuLi, followed by addition of MeI, which gave compound **3** in almost quantitative yield.

Oxidative deprotection of **3** was conveniently achieved using $[Ce(NH_4)_2(NO_3)_6]$ (2 equiv) in CH_3CN/H_2O.

The resulting redox-active ligand **4** was converted into its corresponding Pd^{II}-complex **5** by treatment with $[PdCl_2(cod)]$ (1 equiv; cod = 1,5-cyclooctadiene) in CH_3-CN at reflux temperature.

The ^1H NMR spectrum of **2** is characterized by two methoxy resonances (3.67, 3.86 ppm), four signals for the naphthyl fragment, three pyrazol-1-yl resonances (6.34, 7.55, 7.66 ppm), and one characteristic singlet for the C*H*pz_2 proton (8.23 ppm). All chemical shift values agree with previous findings on related compounds,[28] and the

(12) An, Z.; Pan, X.; Liu, X.; Han, X.; Bao, X. *J. Am. Chem. Soc.* **2006**, *128*, 16028–16029.
(13) Bergstad, K.; Grennberg, H.; Bäckvall, J.-E. *Organometallics* **1998**, *17*, 45–50.
(14) Bäckvall, J.-E.; Hopkins, R. B.; Grennberg, H.; Mader, M. M.; Awasthi, A. K. *J. Am. Chem. Soc.* **1990**, *112*, 5160–5166.
(15) Bäckvall, J.-E.; Chowdhury, R. L.; Karlsson, U. *J. Chem. Soc., Chem. Commun.* **1991**, 473–475.
(16) Byström, S. E.; Larsson, E. M.; Åkermark, B. *J. Org. Chem.* **1990**, *55*, 5674–5675.
(17) Grennberg, H.; Faizon, S.; Bäckvall, J.-E. *Angew. Chem., Int. Ed. Engl.* **1993**, *32*, 263–264.
(18) Purse, B. W.; Tran, L.-H.; Piera, J.; Åkermark, B.; Bäckvall, J.-E. *Chem. Eur. J.* **2008**, *14*, 7500–7503.
(19) Dinnebier, R.; Lerner, H.-W.; Ding, L.; Shankland, K.; David, W. I. F.; Stephens, P. W.; Wagner, M. *Z. Anorg. Allg. Chem.* **2002**, *628*, 310–314.
(20) Margraf, G.; Bats, J. W.; Bolte, M.; Lerner, H.-W.; Wagner, M. *Chem. Commun.* **2003**, 956–957.
(21) Wolf, B.; Zherlitsyn, S.; Lüthi, B.; Harrison, N.; Löw, U.; Pashchenko, V.; Lang, M.; Margraf, G.; Lerner, H.-W.; Dahlmann, E.; Ritter, F.; Assmus, W.; Wagner, M. *Phys. Rev. B* **2004**, *69*, 092403.
(22) Wolf, B.; Brühl, A.; Magerkurth, J.; Zherlitsyn, S.; Pashchenko, V.; Brendel, B.; Margraf, G.; Lerner, H.-W.; Wagner, M.; Lüthi, B.; Lang, M. *J. Magn. Magn. Mater.* **2005**, *290−291*, 411–415.
(23) Margraf, G.; Kretz, T.; de Biani, F. F.; Laschi, F.; Losi, S.; Zanello, P.; Bats, J. W.; Wolf, B.; Remović-Langer, K.; Lang, M.; Prokofiev, A.; Assmus, W.; Lerner, H.-W.; Wagner, M. *Inorg. Chem.* **2006**, *45*, 1277–1288.
(24) Kretz, T.; Bats, J. W.; Losi, S.; Wolf, B.; Lerner, H.-W.; Lang, M.; Zanello, P.; Wagner, M. *Dalton Trans.* **2006**, 4914–4921.
(25) Lerner, H.-W.; Margraf, G.; Kretz, T.; Schiemann, O.; Bats, J. W.; Dürner, G.; de Biani, F. F.; Zanello, P.; Bolte, M.; Wagner, M. *Z. Naturforsch.* **2006**, *61b*, 252–264.
(26) Tsui, Y.; Brühl, A.; Removic-Langer, K.; Pashchenko, V.; Wolf, B.; Donath, G.; Pikul, A.; Kretz, T.; Lerner, H.-W.; Wagner, M.; Salguero, A.; Saha-Dasgupta, T.; Rahaman, B.; Valenti, R.; Lang, M. *J. Magn. Magn. Mater.* **2007**, *310*, 1319–1321.
(27) Wolf, B.; Brühl, A.; Pashchenko, V.; Removic-Langer, K.; Kretz, T.; Bats, J. W.; Lerner, H.-W.; Wagner, M.; Salguero, A.; Saha-Dasgupta, T.; Rahaman, B.; Valentí, R.; Lang, M. *C. R. Chim.* **2007**, *10*, 109–115.
(28) Scheuermann, S.; Kretz, T.; Vitze, H.; Bats, J. W.; Bolte, M.; Lerner, H.-W.; Wagner, M. *Chem. Eur. J.* **2008**, *14*, 2590–2601.
(29) Bäckvall, J.-E.; Gogoll, A. *Tetrahedron Lett.* **1988**, *29*, 2243–2246.
(30) Grennberg, H.; Gogoll, A.; Bäckvall, J.-E. *Organometallics* **1993**, *12*, 1790–1793.
(31) Yamamoto, Y.; Ohno, T.; Itoh, K. *Organometallics* **2003**, *22*, 2267–2272.
(32) Otero, A.; Fernández-Baeza, J.; Tejeda, J.; Antiñolo, A.; Carrillo-Hermosilla, F.; Díez-Barra, E.; Lara-Sánchez, A.; Fernández-López, M.; Lanfranchi, M.; Pellinghelli, M. A. *J. Chem. Soc., Dalton Trans.* **1999**, 3537–3539.
(33) Davies, M. W.; Shipman, M.; Tucker, J. H. R.; Walsh, T. R. *J. Am. Chem. Soc.* **2006**, *128*, 14260–14261.
(34) Peterson, L. K.; Kiehlmann, E.; Sanger, A. R.; Thé, K. I. *Can. J. Chem.* **1974**, *52*, 2367–2374.
(35) Thé, K. I.; Peterson, L. K. *Can. J. Chem.* **1973**, *51*, 422–426.
(36) Thé, K. I.; Peterson, L. K.; Kiehlmann, E. *Can. J. Chem.* **1973**, *51*, 2448–2451.

Scheme 1. Synthesis of the 1,4-Naphthoquinone-Substituted Bis(pyrazol-1-yl)methane Ligand **4** and Its Pd^{II}-Complex **5**[a]

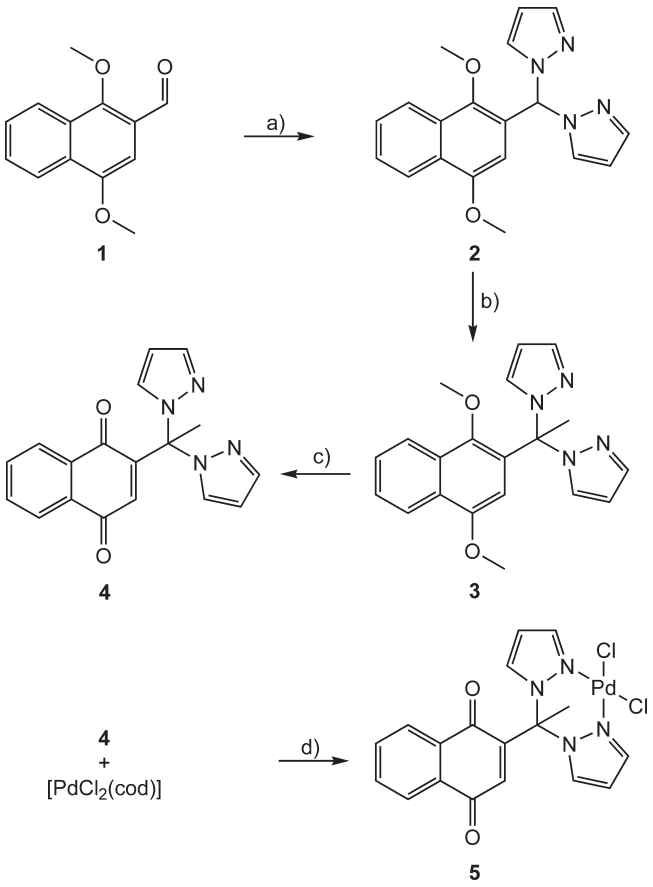

[a] Reagents and conditions: (a) pz_2CO (1 equiv), cat. $CoCl_2$, THF, reflux; (b) (i) *n*BuLi (1 equiv), THF, 0 °C; (ii) MeI (1 equiv), RT; (c) $[Ce(NH_4)_2(NO_3)_6]$ (2 equiv), CH_3CN/H_2O, RT; (d) CH_3CN, reflux.

corresponding integral values are also in accord with the proposed structure of **2** (Scheme 1).

The main difference between the NMR data of compounds **2** and **3** lies in the absence of the C*H*pz_2 proton resonance in the spectrum of **3** and in the presence of a singlet at 2.98 ppm (integrating as 3H) for the newly introduced methyl group ($\delta(^{13}C) = 26.2$).

The successful transformation of **3** into the 1,4-naphthoquinone derivative **4** is proven by the absence of NMR signals assignable to O*C*H_3 substituents and a distinct deshielding of the carbon atoms in positions 1 and 4 of the naphthalene core (**3**: $\delta(^{13}C) = 146.9, 151.8$; **4**: $\delta(^{13}C) = 182.8, 184.9$; the corresponding value in parent 1,4-naphthoquinone is $\delta(^{13}C) = 184.7$[37]). Moreover, upon going from **3** to **4**, we observe a general downfield shift of all carbon resonances assignable to the two six-membered rings, which parallels the trend between the ^{13}C NMR spectra of 1,4-dimethoxynaphthalene[38] on the one hand and 1,4-naphthoquinone[37] on the other.

As to be expected, the NMR-spectra of the Pd^{II}-complex **5** resemble those of the free ligand **4**. However, we note a characteristic downfield shift accompanied by a broadening of both pz-C3,5 resonances upon complexation (**4**: 129.4, 140.1 ppm (in [D_7]DMF, cf. Supporting Information); **5**: 134.8, 144.8 ppm).

To exclude decomplexation of Pd^{II} in DMF solutions of **5** at elevated temperatures, NMR samples of **5** in [D_7]DMF (with or without added LiCl and H_2O) were heated up to 100 °C for 10 min. The spectra recorded before and after temperature treatment always proved to be identical to each other.

X-ray Crystallography. Details of the X-ray crystal structure analyses of **2**, **4**, and **5** are compiled in Table 1.

Compound **2** crystallizes from hexane/EtOAc in the triclinic space group $P\bar{1}$ with two crystallographically independent molecules in the asymmetric unit ($\mathbf{2_A}$ and $\mathbf{2_B}$).

Differences in the key structural parameters of $\mathbf{2_A}$ and $\mathbf{2_B}$ are largely within the margins of experimental error and therefore do not merit further discussion. Thus, only the molecular structure of $\mathbf{2_A}$ is considered here (Figure 1). In line with the NMR spectroscopic results, $\mathbf{2_A}$ is found to contain a bis(pyrazol-1-yl)methyl substituent attached to the 2-position of a 1,4-dimethoxynaphthalene molecule. The bond lengths in the six-membered ring bearing the two methoxy groups lie in the narrow interval between 1.377(2) Å (C3−C4) and 1.436(2) Å (C4−C5); a similar range of C−C distances is observed for the annelated benzene ring (C7−C8 = 1.374(2) Å, C6−C7 = 1.425(2) Å). The C31−O1 vector points almost perpendicular to the naphthalene moiety (C2−C1−O1−C31 = −99.9(1)°), whereas the C32−O2 vector is located in the plane of the aromatic system (C3−C4−O2−C32 = −7.2(2)°). These different conformations of the two methoxy substituents are due to steric repulsion between C31 and the bis(pyrazol-1-yl)methyl fragment and account for a slightly shorter C4−O2 bond (1.371(2) Å) in comparison to the C1−O1 bond (1.386(1) Å). The planes of the two pyrazol-1-yl rings in $\mathbf{2_A}$ include a dihedral angle of 74.6°; the electron lone pairs at N12 and N22 are pointing into opposite directions.

Ligand **4** crystallizes from hexane/EtOAc in the form of yellow plates (monoclinic space group $P2_1/n$; Figure 2).

Its molecular structure shows the newly introduced CH_3 substituent on C11 and no CH_3 groups on O1 and O2. Compared to $\mathbf{2_A}$, the C1−O1 (1.222(2) Å) and the C4−O2 (1.229(2) Å) bonds are shorter by 0.164(2) Å and 0.142(2) Å, respectively. Moreover, a pronounced variation of C−C bond lengths is evident in the substituted six-membered ring (C2−C3 = 1.343(2) Å, C5−C6 = 1.406(2) Å vs C1−C2 = 1.501(2) Å, C1−C6 = 1.489(2) Å, C3−C4 = 1.482(2) Å, C4−C5 = 1.485(2) Å). These latter structural features confirm the conclusions drawn from the NMR spectra of **4**, namely, that the compound is in its 1,4-naphthoquinone oxidation state.

Complex **5** possesses a square-planar configuration with a *cis*-$PdCl_2$ fragment being chelated by the bis(pyrazol-1-yl)methane ligand (Figure 3).

The bond lengths and angles about the Pd^{II}-ion as well as the structural parameters of the bis(pyrazol-1-yl)-methane ligand agree nicely with the corresponding values in the related Pd^{II}-complex [(Ph_2Cpz_2)$PdCl_2$][39] on the one hand and in **4** on the other. As an important structural feature we note that **5** is able to adopt a

(37) Hesse, M.; Meier, H.; Zeeh, B. *Spektroskopische Methoden in der organischen Chemie*; Thieme: Stuttgart, 1987.

(38) SDBS Website: http://riodb01.ibase.aist.go.jp/sdbs/ (National Institute of Advanced Industrial Science and Technology).

(39) Tsuji, S.; Swenson, D. C.; Jordan, R. F. *Organometallics* **1999**, *18*, 4758–4764.

Table 1. Selected Crystallographic Data and Structure Refinement Details for **2**, **4**, and **5**

	2	**4**	**5**
formula	$C_{19}H_{18}N_4O_2$	$C_{18}H_{14}N_4O_2$	$C_{18}H_{14}Cl_2N_4O_2Pd \times {}^4/_3C_2H_3N$
fw	334.37	318.33	550.37
color, shape	colorless, block	yellow, plate	yellow, rod
temp (K)	173(2)	173(2)	165(2)
radiation	MoK_α, 0.71073 Å	MoK_α, 0.71073 Å	MoK_α, 0.71073 Å
crystal system	triclinic	monoclinic	trigonal
space group	$P\bar{1}$	$P2_1/n$	$R3c$
a (Å)	10.4274(6)	8.6041(6)	23.3444(17)
b (Å)	10.9471(6)	17.0313(11)	23.3444(17)
c (Å)	16.2952(10)	11.4378(8)	21.1904(16)
α (deg)	73.329(5)	90	90
β (deg)	73.970(5)	111.777(5)	90
γ (deg)	74.984(5)	90	120
V (Å^3)	1679.63(17)	1556.47(18)	10000.8(13)
Z	4	4	18
$D_{calcd.}$ (g cm^{-3})	1.322	1.358	1.645
F(000)	704	664	4956
μ (mm^{-1})	0.089	0.092	1.104
cryst size (mm)	0.42 × 0.38 × 0.34	0.31 × 0.24 × 0.09	0.65 × 0.14 × 0.11
no of rflns coll	34734	22280	42560
no of indep rflns (R_{int})	7731 (0.0736)	2917 (0.0744)	6496 (0.0386)
data/restr/params	7731/0/455	2917/0/218	6496/1/286
GOOF on F^2	1.025	1.031	1.029
*R*1, *wR*2 ($I > 2\sigma(I)$)	0.0446, 0.1178	0.0371, 0.0956	0.0245, 0.0412
*R*1, *wR*2 (all data)	0.0495, 0.1215	0.0416, 0.0986	0.0345, 0.0438
largest diff peak and hole (e Å^{-3})	0.304, −0.292	0.235, −0.211	0.377, −0.518

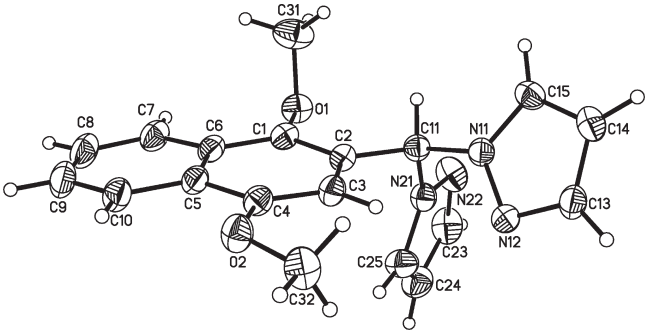

Figure 1. Molecular structure and numbering scheme of compound $\mathbf{2_A}$ (50% displacement ellipsoids). Selected bond lengths [Å], bond angles [deg] and torsion angles [deg]: C1−O1 1.386(1), C4−O2 1.371(2), C1−C2 1.378(2), C1−C6 1.426(2), C2−C3 1.422(2), C3−C4 1.377(2), C4−C5 1.436(2), C5−C6 1.426(2), C2−C11 1.523(2), C11−N11 1.464(2), C11−N21 1.459(2); C2−C11−N11 115.0(1), C2−C11−N21 110.3(1), N11−C11−N21 110.8(1); C2−C1−O1−C31 −99.9(1), C3−C4−O2−C32 −7.2(2).

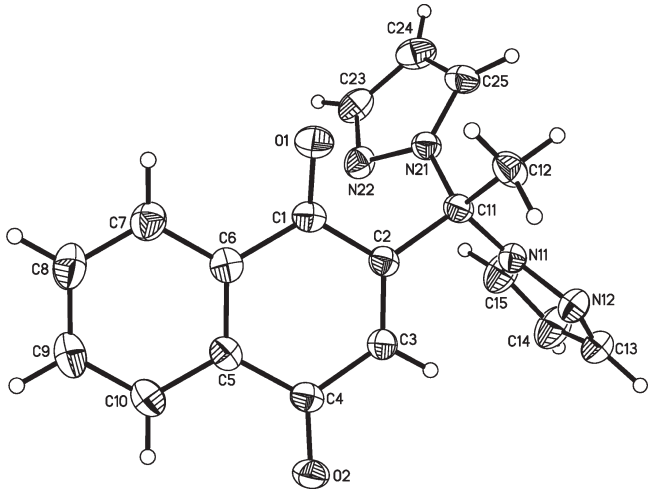

Figure 2. Molecular structure and numbering scheme of compound **4** (50% displacement ellipsoids). Selected bond lengths [Å] and bond angles [deg]: C1−O1 1.222(2), C4−O2 1.229(2), C1−C2 1.501(2), C1−C6 1.489(2), C2−C3 1.343(2), C3−C4 1.482(2), C4−C5 1.485(2), C5−C6 1.406(2), C2−C11 1.533(2), C11−N11 1.480(2), C11−N21 1.465(2); C2−C11−C12 112.1(1), C2−C11−N11 109.8(1), C2−C11−N21 107.0(1), N21−C11−N11 106.4(1), C12−C11−N11 109.7(1), C12−C11−N21 111.5(1).

conformation that brings the Pd^{II}-ion into close proximity to the π face of the NQ moiety (Pd1···C2 = 3.126 Å). A through-space electronic communication between the metal center and the redox-active substituent can therefore be considered a realistic option.[40]

Cyclic Voltammetry. Compounds **4** and **5** were investigated by cyclic voltammetry (DMF, 0 °C, $[NBu_4]PF_6$ (0.1 M) as supporting electrolyte, vs FcH/FcH^+).

The cyclic voltammogram (CV) of the 1,4-naphthoquinone ligand **4** reveals two redox events (Figure 4a), which are assigned to the 1,4-naphthoquinone → 1,4-naphthosemiquinonate → 1,4-naphthohydroquinonate reductions (*Note*: All charges assigned to electrochemically generated products are to be considered formal values since we cannot make safe statements on the degree of protonation of these species). The first electron transition occurs at a potential of $E_{1/2}$ = −0.98 V and shows features of electrochemical reversibility, that is, the current ratio (i_{pc}/i_{pa}) is equal to 1, the current function $i_{pa}/v^{1/2}$ remains constant, and the peak-to-peak separation (ΔE = 94 mV) does not deviate significantly from the value found for the internal ferrocene standard (ΔE(FcH) = 84 mV). The second reduction is irreversible ($E_{pc} \approx -1.80$ V) and the associated peak current is slightly smaller than the peak current of the first electron transfer (similar observations

(40) Wasielewski, M. R. *Chem. Rev.* **1992**, *92*, 435–461.

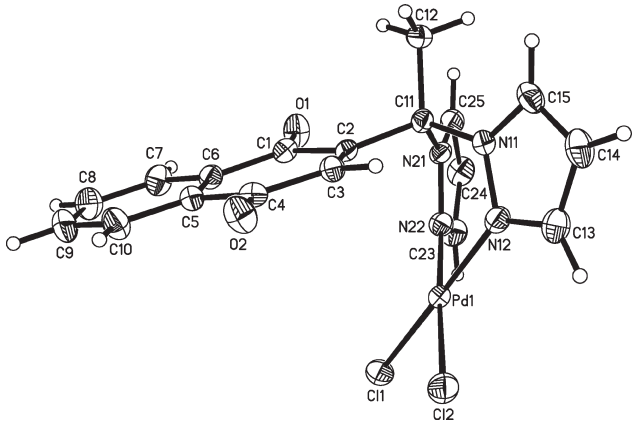

Figure 3. Molecular structure and numbering scheme of compound **5** (50% displacement ellipsoids). Selected bond lengths [Å] and bond angles [deg]: Pd1−Cl1 2.278(1), Pd1−Cl2 2.282(1), Pd1−N12 2.020(2), Pd1−N22 2.011(2), C1−O1 1.219(2), C4−O2 1.223(2), C1−C2 1.499(3), C1−C6 1.491(3), C2−C3 1.347(3), C3−C4 1.470(3), C4−C5 1.482(3), C5−C6 1.399(3); Cl1−Pd1−Cl2 92.1(1), Cl1−Pd1−N22 89.6(1), Cl2−Pd1−N12 90.5(1), N12−Pd1−N22 87.8(1).

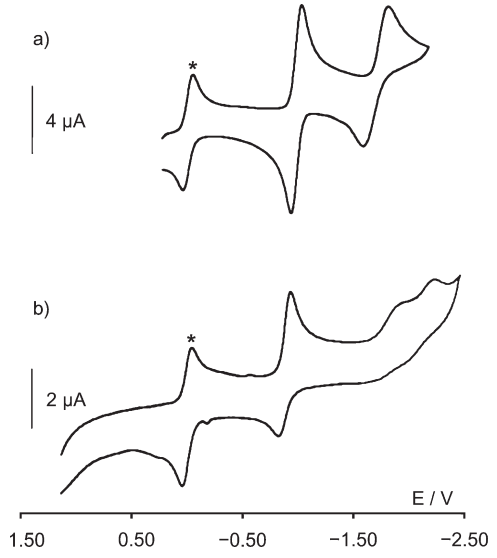

Figure 4. Cyclic voltammograms of (a) **4** and (b) **5**. DMF solutions, 0 °C, $[NBu_4]PF_6$ (0.1 M), scan rates 200 mV s^{-1}, vs FcH/FcH^+ (*).

have already been reported for other 1,4-benzoquinone derivatives[28,41,42]).

The redox potentials of **4** ($E_{1/2} = -0.98$ V, $E_{pc} \approx -1.80$ V) are cathodically shifted compared to the redox potentials of the analogous 1,4-benzoquinone (BQ) ligand BQ-$C(CH_3)pz_2$ ($E_{1/2} = -0.79$ V, -1.53 V; CH_3CN, $[NBu_4]PF_6$ (0.1 M), vs FcH/FcH^+).[28] This different behavior results as a consequence of the annelated benzene ring in **4** because its π-electron system is perturbed to a lesser degree in the oxidized than in the reduced state of the system.[43]

The Pd^{II}-complex **5** gives rise to three redox events (Figure 4b). The half-wave potential of the first transition ($E_{1/2} = -0.88$ V) is close to that of the free ligand ($E_{1/2} = -0.98$ V) and thus attributable to the reduction of the NQ moiety to its 1,4-naphthosemiquinonate form. Contrary to **4**, this first reduction of **5** appears to be quasi-reversible: While the corresponding ΔE value of 130 mV is still similar to that of the internal ferrocene standard (ΔE(FcH) = 120 mV), the current ratio is significantly higher than 1 ($i_{pc}/i_{pa} \approx 1.7$; the same behavior is observed if the sweep is reversed at an applied voltage of -1.38 V). We explain this finding by assuming chemical side reactions of the 1,4-naphthosemiquinonate radical after it has been generated so that not all of it is accessible for reoxidation in the back scan.

The other two redox waves in the CV of **5** show features of irreversibility ($E_{pc} \approx -1.92$ V, -2.24 V) and are assigned to the 1,4-naphthosemiquinonate → 1,4-naphthohydroquinonate transition and to the reduction of the Pd^{II}-center. Again, the redox potentials of **5** ($E_{1/2} = -0.88$ V; $E_{pc} \approx -1.92$ V, -2.24 V) can be compared to those of an analogous 1,4-benzoquinone-containing Pd^{II}-complex $[(BQ\text{-}C(CH_3)pz_2)PdCl_2]$: The CV of the reference compound is characterized by a reversible electron transition at $E_{1/2} = -0.69$ V and a broad and irreversible wave at $E_{pc} \approx -1.58$ V (CH_3CN, $[NBu_4]PF_6$ (0.1 M), vs FcH/FcH^+).[28]

UV−vis Spectro-Electrochemistry. For our projected studies of a Pd-to-NQ electron transfer, we need to be able to distinguish the different oxidation states of the organic redox-active unit in solution. With knowledge of the redox potentials of **4** and **5**, it is now possible to specifically generate certain reduced states of these compounds by electrochemical means and to identify their characteristic signatures in the corresponding UV−vis spectra. Given that the two most cathodic redox waves of **5** are not cleanly resolved and show features of irreversibility, we restricted our investigations to the 1,4-naphthosemiquinonate forms of **4** and **5** because these are the only reduced species that can be generated with appropriate selectivity.

The electronic spectra of the free ligand **4** and its Pd^{II}-complex **5** are rather similar to each other and exhibit bands at $\lambda_{max} = 333$ nm (2950 $L \cdot mol^{-1} \cdot cm^{-1}$) in the case of **4** and 307 nm (4350 $L \cdot mol^{-1} \cdot cm^{-1}$; with a shoulder at ca. 340 nm) in the case of **5**.

To acquire UV−vis data also of the partially reduced species $[\mathbf{4}]^{\bullet-}$ and $[\mathbf{5}]^{\bullet-}$, we generated these semiquinonate radicals by controlled potential electrolysis and recorded their UV−vis spectra *in situ*. Exhaustive one-electron electrochemical reduction of **4** was carried out at an applied potential of $E_w = -1.42$ V. Figure 5a illustrates the development of the absorption bands as a function of time (and injected charge fraction). Upon electrochemical conversion of **4**, its absorption band at $\lambda_{max} = 333$ nm (red curve) continuously decreases and several new bands appear instead ($\lambda_{max} = 303$ nm, 390 nm, 410 nm, 478 nm, 560 nm; black curves). The presence of two isosbestic points at $\lambda = 316$ and 351 nm indicates a clean conversion from **4** to $[\mathbf{4}]^{\bullet-}$ without formation of intermediates or byproducts.

The UV−vis absorption spectra obtained after exhaustive one-electron reduction ($E_w = -1.20$ V) of the Pd^{II}-complex **5** at three different concentrations are depicted in Figure 5b (black curves; the red curve represents the absorption spectrum of the starting material **5**). At low

(41) Prince, R. C.; Dutton, P. L.; Bruce, J. M. *FEBS Lett*. **1983**, *160*, 273–276.
(42) Bauscher, M.; Nabedryk, E.; Bagley, K.; Breton, J.; Mäntele, W. *FEBS Lett*. **1990**, *261*, 191–195.
(43) Peover, M. E. *J. Chem. Soc*. **1962**, 4540–4549.

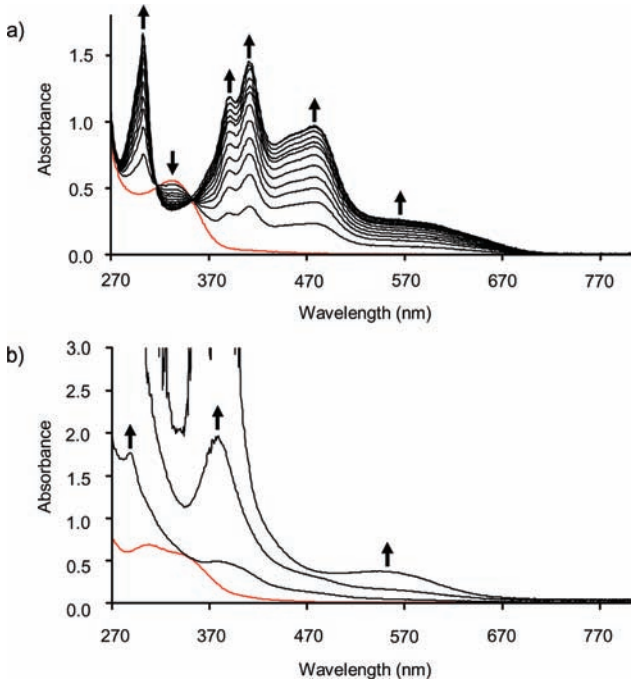

Figure 5. UV−vis absorbance spectra recorded during controlled potential electrolysis. Red curves: spectra of the respective starting material. (a) Exhaustive reduction of **4** (1.43×10^{-4} M; $E_w = -1.42$ V; 0 to 20 min); (b) exhaustive reduction of **5** (spectra recorded at the end-points of electrolysis at three different starting concentrations of **5** (1.1×10^{-4} M, 2.2×10^{-4} M, 3.3×10^{-4} M; $E_w = -1.20$ V). Conditions: DMF, 0 °C, $[NBu_4]PF_6$ (0.1 M)).

concentrations of the radical anion $[\mathbf{5}]^{\bullet-}$, its UV−vis spectrum is characterized by an absorption band at $\lambda_{max} = 290$ nm with a shoulder at $\lambda_{max} \approx 375$ nm. This shoulder becomes a well-resolved signal when the concentration is increased. Finally, at the highest of the chosen concentrations an additional broad absorption band is clearly detectable at $\lambda_{max} \approx 550$ nm.

Since we can only roughly estimate the concentrations of the reduced species $[\mathbf{4}]^{\bullet-}$ and $[\mathbf{5}]^{\bullet-}$, we refrain from calculating their extinction coefficients.

Chemical Reduction of 5 with Triethylamine. The previously described experiments constitute a firm basis for investigating a possible electron transfer between the transition metal center and the organic redox system in complexes with **4**-type ligands.

Starting from complex **5**, which contains both its electroactive units in their oxidized states, we first selectively reduced the Pd^{II}-center to Pd^0 and then looked for the signature of the 1,4-naphthosemiquinonate radical in the UV−vis spectrum of the reaction mixture. Triethylamine (NEt_3) appeared to be the reducing agent of choice, since it is commonly used to generate Pd^0-species from Pd^{II}-precursors in Pd-catalyzed reactions.[44]

(44) In reactions requiring Pd^0 (e.g., Pd-catalyzed Heck reaction), formation of the active complex from its Pd^{II}-precursor is often achieved with NEt_3. The generally accepted mechanism of this two-electron reduction involves (i) coordination of NEt_3, (ii) β-hydride elimination (with liberation of an iminium ion), and (iii) reductive elimination of HX from Pd^{II} (cf. Clayden, J.; Greeves, N.; Warren, S.; Wothers, P. *Organic Chemistry*; Oxford University Press Inc.: New York, 2001). Given this background, we assume a two-electron process also in our case, even though an accompanying single-electron transfer from NEt_3 to Pd^{II} cannot entirely be excluded.

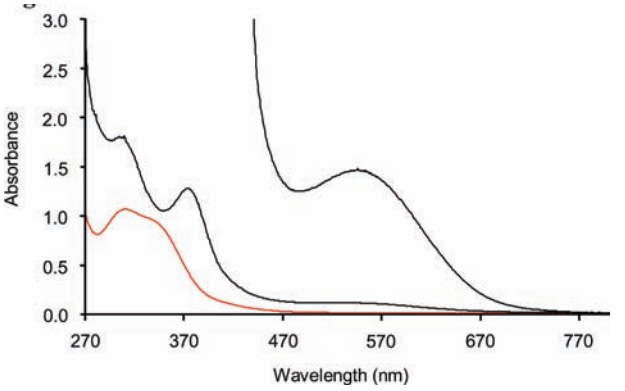

Figure 6. UV−vis absorbance spectra of a mixture of **5** and excess NEt_3 in DMF before (red curve) and after heating to 100 °C, 5 min at two different starting concentrations of **5** (black curves).

To make sure that NEt_3 does not react with the ligand in the absence of a transition metal ion, a mixture of **4** and exc. NEt_3 in DMF was kept at 100 °C for 10 min. After cooling to room temperature (RT), the UV−vis spectrum of the mixture was still virtually identical to that of **4** (cf. Figure 1S in the Supporting Information). The experiment had a different outcome under photolytic conditions ($\lambda_{irr} = 254$ nm, 8 W, 10 min) which led to the appearance of a new broad band at $\lambda_{max} \approx 470$ nm (cf. Figure 1S and Scheme 1S in the Supporting Information). This result did not come as a surprise because it is known that photoexcited unsaturated compounds (among them 1,4-quinones) tend to undergo redox-reactions with amines.[45] Given this background, we feel safe to assume that NEt_3 is indeed a suitable selective reducing agent for the Pd^{II}-center in **5** as long as the reaction mixture is carefully protected from light.

In the key experiments to elucidate a $Pd^0 \rightarrow$ NQ charge transfer, mixtures of **5** and excess NEt_3 in DMF were heated to 100 °C under strict exclusion of light. UV−vis spectra were recorded at RT after 5 min reaction time on solutions of two different concentrations (Figure 6, black curves; red curve: absorption spectrum of **5**). Three absorption bands, at $\lambda_{max} = 300$ nm, 370 nm, and ≈ 550 nm, can unambiguously be identified.

A comparison of these spectra with those of the electrochemically generated 1,4-naphthosemiquinonate radical $[\mathbf{5}]^{\bullet-}$ (Figure 5b; $\lambda_{max} = 290$, 375, 550 nm) reveals a good match in band positions and shapes. This leads to the conclusion, that, after reduction of the Pd^{II}-center in **5**, one electron is transferred from the resulting Pd^0-atom to the 1,4-naphthoquinone ligand, which in turn adopts the 1,4-naphthosemiquinonate form.

EPR Spectroscopy. The interpretation of the UV−vis spectroscopic results was further confirmed by EPR measurements. The EPR spectrum of a reaction mixture of **5** and excess triethylamine, similarly prepared and treated as described above, exhibits a signal with a *g*-value of 2.0046, which is split into a doublet because of hyperfine coupling to a single proton (Figure 7). The experimental spectrum was simulated with $A_H = 3.8$ G.

We assign this signal to an unpaired electron in the π-system of the NQ fragment because its g-value is in the

(45) Cohen, S. G.; Parola, A.; Parsons, G. H., Jr. *Chem. Rev.* **1973**, *73*, 141–161.

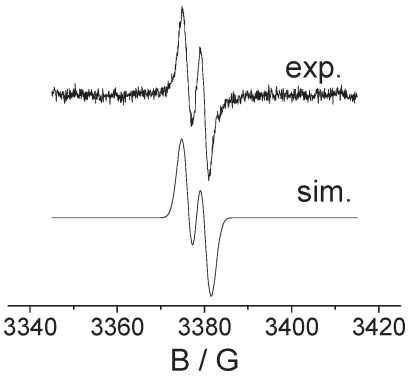

Figure 7. X-band EPR spectrum of a reaction mixture of **5** and excess NEt_3 in DMF after heating to 100 °C (5 min) and its simulation.

typical range for organic radicals. Judging from the hyperfine splitting, the unpaired electron seems to be predominantly located in that part of the ring system that carries the oxygen substituents (and bears only one proton).

We note in this context, that an EPR blank test on a mixture of the free ligand **4** with excess NEt_3 in in DMF showed no signal after temperature treatment.

The absence of an EPR signal assignable to a Pd^I-species is plausible given the pronounced tendency of Pd^I-ions to form stable closed shell Pd−Pd dimers.[46]

Conclusions

In numerous Pd-catalyzed organic transformations, a Pd^0-intermediate has to be reoxidized to close the catalytic cycle. 1,4-Benzoquinone (BQ) is a popular electron acceptor in this context and known to initially coordinate the Pd^0-atom via the olefinic bond(s).

For obvious reasons it would be desirable to replace this two-component mixture by a single-component system combining the active Pd-site and the redox co-catalyst in one molecule. To identify promising lead structures, it has first to be clarified whether or not the covalent Pd-BQ interaction provides the exclusive pathway for efficient metal-to-ligand charge transfer. To answer this question, we equipped a chelating bis(pyrazol-1-yl)methane ligand with a 1,4-naphthoquinone (NQ) substituent, prepared the corresponding [(N^N)$PdCl_2$] complex and proved its thermal stability in DMF solution up to temperatures of 100 °C.

Even though neither intra- nor intermolecular Pd-NQ coordination is likely to take place in this molecule, we nevertheless observed the spectroscopic signature (UV−vis, EPR) of a 1,4-naphthosemiquinonate radical immediately after selective $Pd^{II} \rightarrow Pd^0$ reduction using NEt_3 in DMF. This result indicates that the formation of a Pd^0-BQ complex is not a prerequisite for a successful reoxidation process, but that the electrons can also be transferred via a through-space pathway (or, less likely, via σ-bonds of the ligand framework).

However, it should be noted that the signal-to-noise ratio in the EPR spectrum points toward a low concentration of the paramagnetic organic species. Probably, the reduction of Pd^{II} by NEt_3 constitutes the bottleneck of the overall electron transfer because NMR spectra recorded on mixtures of [(N^N)$PdCl_2$] and NEt_3 in DMF after heating for 10 min still showed large amounts of unreacted starting material.[47] This problem is, however, specific to our model system and not relevant for real catalytic applications. Moreover, 1,4-naphthoquinone is a weaker electron acceptor than 1,4-benzoquinone and, again only in our special case where NEt_3 has to be present, Pd → NQ electron transfer might be hampered by the lack of protons required for the formation of charge-neutral 1,4-naphthosemiquinone.

In summary, we propose 1,4-quinone-substituted bis-(pyrazol-1-yl)methanes as promising ligands for the development of hybrid Pd-catalysts that mediate aerobic oxidation reactions.

Experimental Part

General Procedures. All reactions and manipulations of air-sensitive compounds were carried out in dry, oxygen-free nitrogen by using standard Schlenk ware. Tetrahydrofuran (THF) was freshly distilled under argon from Na/benzophenone. 1,4-Dimethoxy-2-naphthalenecarboxaldehyde[33] and bis(pyrazol-1-yl)-methanone[36] were synthesized according to literature procedures.

NMR spectra were recorded at 27 °C with Bruker AM-250, Bruker Avance-300, and Bruker Avance-400 spectrometers. Chemical shifts are referenced to residual solvent signals ($^1H/^{13}C\{^1H\}$: $CDCl_3$: 7.26/77.16; [D_7]DMF: 7.95/162.29). Abbreviations: s = singlet; d = doublet; t = triplet; vt = virtual triplet; dd = doublet of doublets; br = signal broadened; m = multiplet; n.r. = multiplet expected in the ^1H NMR spectrum, but not resolved; pz = pyrazol-1-yl; NHQ = 1,4-naphthohydroquinone core; NQ = 1,4-naphthoquinone core.

Elemental analyses were performed by the Microanalytical Laboratory of the University of Frankfurt. Mass spectra were recorded with a Fisons VG PLATFORM II-(ESI) and a Fisons TofSpec-mass spectrometer (MALDI).

UV−vis Spectroscopy. UV−vis spectra were recorded on a Varian Cary 50 UV−vis spectrophotometer. For spectro-electrochemical measurements, the spectrometer was equipped with a Hellma 661.500 quartz immersion probe.

Electrochemistry. Cyclic voltammograms were recorded using an EG&G Princeton Applied Research 263A potentiostat with a platinum disk working electrode. Carefully dried (calciumhydride) and degassed *N*,*N*-dimethylformamide (DMF) was used as the solvent and [NBu_4]PF_6 as the supporting electrolyte (0.1 M). All potential values are referenced against the FcH/FcH^+ couple. Bulk electrolysis was performed at 0 °C using a platinum-net electrode.

EPR Spectroscopy. EPR spectra in the X band were recorded with a Bruker System EMX connected with an ER 4131 VT variable temperature accessory. EPR simulations were done using the Simfonia software of Bruker.

Synthesis of 2. A solution of 1,4-dimethoxy-2-naphthalenecarboxaldehyde (3.010 g, 13.92 mmol) in THF (50 mL) was treated with bis(pyrazol-1-yl)methanone (2.260 g, 13.94 mmol) and anhydrous $CoCl_2$ (0.030 g, 0.23 mmol). The reaction mixture was kept at reflux temperature for 7 h and then allowed to cool to RT. After the addition of H_2O (50 mL), the product was extracted into CH_2Cl_2 (3 × 50 mL). The combined organic phases were dried ($MgSO_4$), filtered and the filtrate was evaporated to dryness *in vacuo*. Flash column chromatography yielded the pure product as colorless solid (3.951 g, 85%). Single crystals of **2** were grown from hexane/EtOAc (3:1) by slow evaporation of the solvents at RT.

(46) Murahashi, T.; Nakashima, H.; Nagai, T.; Mino, Y.; Okuno, T.; Jalil, M. A.; Kurosawa, H. *J. Am. Chem. Soc.* **2006**, *128*, 4377–4388.

(47) This reduction reaction proceeds via β-hydride elimination from Pd-coordinated NEt_3. It is known that the tendency to β-hydride elimination is rather small for Pd^{II}-complexes with bidentate nitrogen ligands (e.g., 2,2′-bipyridine, diimines; cf. ref. 11, p. 263).

R_f = 0.15 (silica gel; hexane/EtOAc (3:1)). ^{1}H NMR (250.1 MHz, $CDCl_3$): δ = 3.67, 3.86 (2 × s, 2 × 3H; OMe), 6.34 (vt, 2H; pz-H4), 6.65 (s, 1H; NHQ-H3), 7.49−7.60 (m, 2H; NHQ-H6,7), 7.55, 7.66 (n.r., d, 2 × 2H; pz-H3,5), 8.01−8.09, 8.21−8.28 (2 × m, 2 × 1H; NHQ-H5,8), 8.23 (s, 1H; $CHpz_2$). ^{13}C NMR (62.9 MHz, $CDCl_3$): δ = 55.7, 62.7 (OMe), 73.0 ($CHpz_2$), 101.7 (NHQ-C3), 106.5 (pz-C4), 122.4, 122.7 (NHQ-C5,8), 124.1 (NHQ-C*), 126.7, 127.2 (NHQ-C6,7), 127.4, 128.3 (NHQ-C*), 129.8, 141.0 (pz-C3,5), 147.8, 152.6 (NHQ-C1,4); C* = C2 or 9 or 10. Anal. Calcd for $C_{19}H_{18}N_4O_2$ [334.37]: C, 68.25; H, 5.43; N, 16.76. Found: C, 68.54; H, 5.48; N, 16.49%. MALDI-MS m/z: 334 ($[M]^+$).

Synthesis of 3. A solution of *n*BuLi in hexane (1.6 M, 1.3 mL; 2.08 mmol) was added at 0 °C via syringe to a stirred solution of **2** (0.700 g, 2.09 mmol) in THF (20 mL). After 30 min, the resulting reddish solution was allowed to warm to RT, and MeI (0.297 g, 2.09 mmol) was added. Stirring was continued for 30 min, H_2O (30 mL) was added to the reaction mixture, and **3** was extracted into CH_2Cl_2 (3 × 50 mL). The combined organic phases were dried over $MgSO_4$, filtered and the filtrate was evaporated to dryness *in vacuo*. The remaining brown oil was purified by flash column chromatography to yield a colorless solid (0.714 g, 98%).

R_f = 0.40 (silica gel; hexane/EtOAc (2:1)). ^{1}H NMR (250.1 MHz, $CDCl_3$): δ = 2.98 (s, 3H; Me), 3.37, 3.66 (2 × s, 2 × 3H; OMe), 5.26 (s, 1H; NHQ-H3), 6.36 (vt, 2H; pz-H4), 7.39 (d, $^3J_{HH}$ = 2.5 Hz, 2H; pz-H3 or 5), 7.44−7.55 (m, 2H; NHQ-H6,7), 7.69 (d, $^3J_{HH}$ = 1.3 Hz, 2H; pz-H5 or 3), 7.95−8.02, 8.17−8.24 (2 × m, 2 × 1H; NHQ-H5,8). ^{13}C NMR (62.9 MHz, $CDCl_3$): δ = 26.2 (Me), 55.2, 61.2 (2 × OMe), 82.4 (*C*Mepz$_2$) 102.0 (NHQ-C3), 106.3 (pz-C4), 122.5, 122.7 (NHQ-C5,8), 126.1, 126.7 (NHQ-C6,7), 127.1, 128.9 (NHQ-C*), 129.7 (pz-C3 or 5), 130.6 (NHQ-C*), 140.1 (pz-C5 or 3), 146.9, 151.8 (NHQ-C1,4); C* = C2 or 9 or 10. Anal. Calcd for $C_{20}H_{20}N_4O_2$ [348.40]: C, 68.95; H, 5.79; N, 16.08. Found: C, 68.98; H, 5.89; N, 16.22%. ESI-MS m/z: 281 ($[M - pz]^+$).

Synthesis of 4. A solution of $[Ce(NH_4)_2(NO_3)_6]$ (2.204 g, 4.02 mmol) in CH_3CN (20 mL) was added to a solution of **3** (0.700 g, 2.01 mmol) in CH_3CN (20 mL). After the mixture had been stirred for 30 min, H_2O (10 mL) was added and stirring continued for 2 h. **4** was extracted into CH_2Cl_2 (4 × 50 mL), the combined organic phases were dried over $MgSO_4$ and filtered. Silica gel was added to the orange filtrate, the solvent was carefully evaporated, the remaining orange powder placed on top of a pad of silica gel and flushed with hexane/EtOAc (2:1). The filtrate was evaporated *in vacuo* to yield pure **4** as yellow solid (0.210 g, 33%), which tends to turn greenish upon prolonged exposure to air. Single crystals of **4** were grown from hexane/EtOAc (2:1) by slow evaporation of the solvents at RT.

^{1}H NMR (300.0 MHz, $CDCl_3$): δ = 2.79 (s, 3H; Me), 5.67 (s, 1H; NQ-H3), 6.38 (dd, $^3J_{HH}$ = 1.8 Hz, 2.4 Hz, 2H; pz-H4), 7.44, 7.61 (2 × d, $^3J_{HH}$ = 2.4 Hz, 1.8 Hz, 2 × 2H; pz-H3,5), 7.69−7.75 (m, 2H; NQ-H6,7), 7.98−8.06 (m, 2H; NQ-H5,8). ^{13}C NMR (75.5 MHz, $CDCl_3$): δ = 25.4 (Me), 80.2 (*C*Mepz$_2$), 107.4 (pz-C4), 126.2, 127.2 (NQ-C5,8), 128.5 (pz-C3 or 5), 131.9, 132.7 (NQ-C*), 134.0, 134.2 (NQ-C6,7), 135.1 (NQ-C3), 140.3 (pz-C5 or 3), 150.1 (NQ-C*), 182.8, 184.9 (NQ-C1,4); C* = C2 or 9 or 10. Anal. Calcd for $C_{18}H_{14}N_4O_2$ [318.33]: C, 67.91; H, 4.43; N, 17.60. Found: C, 68.10; H, 4.62; N, 17.76%. ESI-MS m/z: 251 ($[M - pz]^+$). UV−vis λ_{max} (ε): 333 nm (2950 L·mol^{-1}·cm^{-1}).

Synthesis of 5. Neat $[PdCl_2(cod)]$ (0.089 g, 0.31 mmol) was added to a solution of **4** (0.100 g, 0.31 mmol) in CH_3CN (20 mL). The reaction mixture was kept at reflux temperature for 30 min, whereupon a yellow precipitate formed, which was collected on a frit and washed with CH_3CN (5 mL), $CHCl_3$ (10 mL), and finally pentane (10 mL). This procedure gave **5** as yellow powder (0.092 g, 60%). Single crystals were obtained by gas-phase diffusion of CH_3CN into a saturated solution of **5** in DMF.

^{1}H NMR (250.1 MHz, [D$_7$]DMF): δ = 2.97 (s, 3H; Me), 5.94 (s, 1H; NQ-H3), 6.72 (br, 2 H; pz-H4), 7.86−7.94 (m, 4H; NQ-H, pz-H3 or 5), 8.01−8.06 (m, 2H; NQ-H), 8.79 (d, $^3J_{HH}$ = 2.8 Hz, 2H; pz-H5 or 3). ^{13}C NMR (62.9 MHz, [D$_7$]DMF): δ = 23.5 (Me), 79.9 (*C*Mepz$_2$), 107.7 (pz-C4), 126.2, 127.0 (NQ-C5,8), 131.8, 132.7 (NQ-C*), 134.8 (br, pz-C3 or 5), 135.0, 135.1 (NQ-C6,7), 138.5 (NQ-C3), 144.8 (br, pz-C5 or 3), 146.7 (NQ-C*), 182.0, 183.8 (NQ-C1,4); C* = C2 or 9 or 10. Anal. Calcd for $C_{18}H_{14}Cl_2N_4O_2Pd$ [495.66]: C, 43.62; H, 2.85; N, 11.30. Found: C, 43.35; H, 2.61; N, 11.44%. ESI-MS m/z: 532 ($[M - Cl + DMF]^+$). UV−vis λ_{max} (ε): 307 nm (4350 L·mol^{-1}·cm^{-1}; with a shoulder at ca. 340 nm).

X-ray Crystallography of 2, 4, and 5. Data collections were performed on a Stoe-IPDS-II two-circle-diffractometer (**2**, **4**) and on a SIEMENS SMART CCD diffractometer (**5**) with graphite-monochromated Mo Kα radiation. In all cases, repeatedly measured reflections remained stable. An empirical absorption correction was performed for **5** using the program SADABS.[48] Equivalent reflections were averaged. The structures were solved by direct methods[49] and refined with full-matrix least-squares on F^2 using the program SHELXL-97.[50] Hydrogen atoms were placed on ideal positions and refined with fixed isotropic displacement parameters using a riding model. Compound **2** crystallizes with two crystallographically independent molecules in the asymmetric unit. Complex **5** crystallizes together with $^4/_3$ equivalents of acetonitrile in the crystal lattice.

Cambridge Crystallographic Data Centre (CCDC) reference numbers: 737849 (**2**), 737850 (**4**), 738399 (**5**).

Acknowledgment. This research was supported by the Deutsche Forschungsgemeinschaft (DFG) and the Fonds der Chemischen Industrie (FCI). S.S. is grateful to the Studienstiftung des deutschen Volkes for a Ph. D. grant.

Supporting Information Available: Crystallographic data of **2**, **4**, and **5** in CIF format; UV−vis spectra of mixtures of **4** and NEt_3 after heating and after irradiation at 254 nm; NMR data of **4** in [D$_7$]DMF. This material is available free of charge via the Internet at http://pubs.acs.org.

(48) Sheldrick, G. M. *SADABS*; University of Göttingen: Göttingen, Germany, 2000.
(49) Sheldrick, G. M. *Acta Crystallogr.* **1990**, *A46*, 467–473.
(50) Sheldrick, G. M. *SHELXL-97. A Program for the Refinement of Crystal Structures*; Universität Göttingen: Göttingen, Germany, 1997.